Stars and their variability observed from space
C. Neiner, W. W. Weiss, D. Baade, R. E. Griffin, C. C. Lovekin, A. F. J. Moffat (eds)

ROTATIONAL INVERSIONS ALONG THE LOWER PART OF THE RED-GIANT BRANCH

F. Ahlborn[1,2], E. P. Bellinger[3], S. Hekker [2,3], S. Basu[4] and G. C. Angelou[1]

Abstract. This poster illustrated the results of an investigation into how the accuracy of internal rotation rates, estimated asteroseismically, change as stellar models with varying mass and metallicity evolve along the red-giant branch. A range of increased sensitivity to the surface rotation just below the red-giant bump was found.

Keywords: Asteroseismology, stars: rotation, oscillations, interiors

1 Introduction

Stellar rotation has a substantial impact on the structure and evolution of a star, as it affects internal processes like rotational mixing and the transport of angular momentum. However, it has been shown that hydrodynamic means of angular momentum transport *as currently included* are not sufficient to reproduce core-rotation rates estimated asteroseismically for stars on the red-giant branch (RGB) (Fuller et al. 2019; Ouazzani et al. 2019; Eggenberger et al. 2017; Spada et al. 2016; Marques et al. 2013; Ceillier et al. 2013; Eggenberger et al. 2012). The internal rotation of a star splits its non-radial oscillation modes into multiplets. The frequency difference between subsequent multiplet components is called *rotational splitting*. The advent of high-precision photometric space missions like *CoRoT* (Baglin et al. 2006) and *Kepler* (Borucki et al. 2008) enabled one to resolve rotational splittings in red-giant stars and to probe their internal rotation rates (Beck et al. 2012; Mosser et al. 2012; Gehan et al. 2018; Beck et al. 2014, 2018). To estimate internal rotation rates as a function of radius, so-called asteroseismic *rotational inversions* have been performed for a number of red giants (Deheuvels et al. 2012, 2014; Di Mauro et al. 2016, 2018; Triana et al. 2017). Our poster described results from a study of the asteroseismic sensitivity to internal rotation along the RGB (Ahlborn et al. 2019, submitted).

2 Synthetic Data and Rotational Inversions

We prepared different synthetic data sets to study the behaviour of asteroseismic rotational inversions along the lower part of the RGB. We constructed five different stellar evolution tracks from the pre-main-sequence to beyond the luminosity bump using Modules for Experiments in Stellar Astrophysics (MESA,version r8845, (Paxton et al. 2019), and references therein). To perform rotational inversions, we selected models from the base of the RGB up to the luminosity bump. We investigated models with inital masses of 1, 1.5 and 2 $M_\odot$, and metallicities of [Fe/H] $= -0.2, 0.0$, and 0.2. We used the stellar oscillation code GYRE (Townsend & Teitler 2013; Townsend et al. 2018) to compute the oscillation frequencies and rotational kernels for the combine the individual rotational kernels linearly from the data set to form so-called *averaging kernels* $K(r, r_0)$ localised at a chosen target-radius r_0. For each selected model we performed a rotational inversion and computed a core-averaging kernel (target radius $r_0/R = 0.003$) and a surface-averaging kernel ($r_0/R = 0.98$), and an estimate of the core- and surface-rotation rates. To analyse the inversion results, we computed the sensitivity of the core-averaging kernel in the core ($\beta_{\rm core}$) and the sensitivity of the surface-averaging kernel in the envelope ($\beta_{\rm surf}$):

$$\beta_{\rm core} = \int_0^{r_{\rm core}} K(r, 0.003)\mathrm{d}r; \quad \beta_{\rm surf} = 1 - \int_0^{r_{\rm core}} K(r, 0.98)\mathrm{d}r\,. \tag{2.1}$$

[1] Max Planck Institute for Astrophysics, Karl-Schwarzschild-Straße 1, 85748 Garching, Germany,
e-mail: fahlborn@mpa-garching.mpg.de
[2] Max Planck Institute for Solar System Research, Justus-von-Liebig-Weg 3, 37077 Göttingen, Germany
[3] Stellar Astrophysics Centre, Department of Physics and Astronomy, Aarhus University, Ny Munkegade 120, DK-8000 Aarhus C, Denmark
[4] Department of Astronomy, Yale University, New Haven, CT 06520, USA

The radius $r_{\rm core}$ indicates the integration boundary between the core and the envelope in terms of the internal rotation profile. It does not need to be the actual radius of the stellar core.

3 Results and Conclusions

The left panel of Fig. 1 shows the core and the surface sensitivities, $\beta_{\rm core}$ and $\beta_{\rm surf}$, for a 1 $M_\odot$ model in blue and red dots, respectively in; the base of the convective envelope was adopted as $r_{\rm core}$. The computed values of the core sensitivities showed that the sensitivity of the core-averaging kernels is almost entirely confined below the base of the convection zone for all models under consideration. This means that the computed core-averaging kernels are well localised at the radius of the chosen target. However, the computed surface sensitivities showed a substantially different behaviour. First they decrease until they reach a minimum at about 19 $L_\odot$. From there on there is a narrow range of increased sensitivity to the surface rotation, just below the luminosity bump. The minimum surface sensitivity of about 70% translates into a 30% sensitivity to the core rotation in the estimated surface-rotation rate. Even at the base of the RGB, the estimated surface-rotation rates showed about a 5% sensitivity to the core rotation.

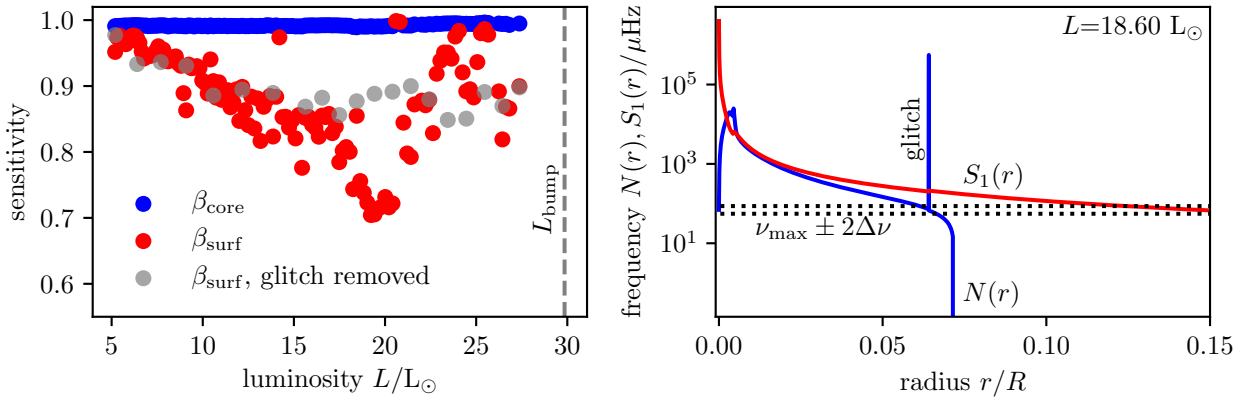

Fig. 1. Left: Core (blue) and surface (red) sensitivities $\beta_{\rm core}$ and $\beta_{\rm surf}$ for a solar metallicity, 1 $M_\odot$ model. Grey dots indicate inversion results for models where the peak associated with the composition discontinuity has been removed manually from the buoyancy frequency. **Right:** Propagation diagram for a 1.0 $M_\odot$ model in the vicinity of the surface-sensitivity minimum. N indicates the buoyancy frequency, and S_1 the Lamb frequency, for $l = 1$ modes. The frequency range of the dipole modes used for the rotational inversions is indicated by two horizontal dotted lines.

The increased surface sensitivity below the bump indicates that there is a theoretical possibility to estimate surface-rotation rates in red giants close to the luminosity bump with an accuracy similar to that at the base of the RGB. The same qualitative behaviour was found for all the masses and metallicities under consideration. The glitch in the buoyancy frequency (Fig. 1, right panel) could be responsible for the decrease and subsequent increase in surface sensitivities. As long as the glitch is in the range of frequencies used, the surface sensitivity decreases. When the glitch moves out of the frequency range, the surface sensitivity increases again. We recomputed some of the rotational inversions for models from the 1 $M_\odot$ track in which we removed the glitch artificially, and found that the minimum in sensitivity is no longer present, and that the overall decrease in surface sensitivity is more gentle (grey dots, left panel of Fig. 1).

The research leading to these results received funding from the European Research Council under the ECs Seventh Framework Programme (FP7/2007-2013)/ERC, grant no. 338251, a "Stellar Ages"). SB acknowledges partial funding from NASA grant NNX16A109G and NSF grant AST-1514676.

References

Baglin, A., Auvergne, M., Barge, P., et al. 2006, in ESA Special Publication, Vol. 1306, The CoRoT Mission Pre-Launch Status - Stellar Seismology and Planet Finding, ed. M. Fridlund, A. Baglin, J. Lochard, & L. Conroy, 33

Beck, P. G., Hambleton, K., Vos, J., et al. 2014, A&A, 564, A36

Beck, P. G., Kallinger, T., Pavlovski, K., et al. 2018, A&A, 612, A22

Beck, P. G., Montalban, J., Kallinger, T., et al. 2012, Nature, 481, 55

Borucki, W., Koch, D., Basri, G., et al. 2008, in IAU Symposium, Vol. 249, Exoplanets: Detection, Formation and Dynamics, ed. Y.-S. Sun, S. Ferraz-Mello, & J.-L. Zhou, 17–24

Ceillier, T., Eggenberger, P., García, R. A., & Mathis, S. 2013, A&A, 555, A54

Deheuvels, S., Doğan, G., Goupil, M. J., et al. 2014, 564, A27

Deheuvels, S., García, R. A., Chaplin, W. J., et al. 2012, ApJ, 756, 19

Di Mauro, M. P., Ventura, R., Cardini, D., et al. 2016, ApJ, 817, 65

Di Mauro, M. P., Ventura, R., Corsaro, E., & Lustosa De Moura, B. 2018, ApJ, 862, 9

Eggenberger, P., Lagarde, N., Miglio, A., et al. 2017, A&A, 599, A18

Eggenberger, P., Montalbán, J., & Miglio, A. 2012, ApJ, 544, L4

Fuller, J., Piro, A. L., & Jermyn, A. S. 2019, MNRAS, 485, 3661

Gehan, C., Mosser, B., Michel, E., Samadi, R., & Kallinger, T. 2018, A&A, 616, A24

Marques, J. P., Goupil, M. J., Lebreton, Y., et al. 2013, A&A, 549, A74

Mosser, B., Goupil, M. J., Belkacem, K., et al. 2012, 548, A10

Ouazzani, R. M., Marques, J. P., Goupil, M. J., et al. 2019, A&A, 626, A121

Paxton, B., Smolec, R., Schwab, J., et al. 2019, ApJSS, 243, 10

Spada, F., Gellert, M., Arlt, R., & Deheuvels, S. 2016, A&A, 589, A23

Townsend, R. H. D., Goldstein, J., & Zweibel, E. G. 2018, MNRAS, 475, 879

Townsend, R. H. D. & Teitler, S. A. 2013, MNRAS, 435, 3406

Triana, S. A., Corsaro, E., De Ridder, J., et al. 2017, A&A, 602, A62